Cellular and Molecular Bioengineering, Vol. 8, No. 3, September 2015 (© 2015) pp. 488–495
DOI: 10.1007/s12195-015-0394-7

Integrins Direct Cell Adhesion in a Substrate-Dependent Manner

ANDREAS P. KOUROUKLIS[1] and HARRY BERMUDEZ[2]

[1]Department of Chemical Engineering, University of Massachusetts, Amherst, MA, USA; and [2]Department of Polymer Science and Engineering, University of Massachusetts, Amherst, MA, USA

(*Received 23 January 2015; accepted 27 April 2015; published online 7 May 2015*)

Associate Editor Michael R. King oversaw the review of this article.

Abstract—The relationship between substrate properties and cell behavior is complex, including roles for both mechanics and biochemistry. Here we investigate the role of viscous dissipation on cell adhesion behaviors, using polymer films of tunable lateral mobility. We find that fibroblasts selectively use $\alpha_v\beta_3$ and $\alpha_5\beta_1$ integrin receptors to control their spreading area and polarization on low and high mobility films, respectively. In addition, the dynamics of cell spreading and polarization are well described by a semi-empirical sigmoidal relationship. Analysis of cell dynamic behavior reveals that spreading dynamics are controlled by the availability of integrins, whereas the polarization dynamics are controlled by intracellular signaling. The result that cells preferentially use specific integrin receptors in response to substrate mechanical properties has broad implications for processes in dynamic environments such as wound healing and cancer metastasis.

Keywords—Block copolymers, Self-assembly, Lateral mobility, Cell behavior, Focal adhesions.

INTRODUCTION

Cell adhesion, spreading, and polarization are directly related with how cells sense their surroundings.[9] Among the many molecules involved,[38] integrin receptors play a central role in the bidirectional signaling between intracellular and extracellular environments.[19] The $\alpha_5\beta_1$ and $\alpha_v\beta_3$ integrins are of particular importance because they bind to extracellular adhesive proteins (including those that contain the RGD peptide sequence).[19,30] The $\alpha_5\beta_1$ and $\alpha_v\beta_3$ integrins are also known to demonstrate both distinct and redundant functionalities in cell adhesion. For example, $\alpha_5\beta_1$ and $\alpha_v\beta_3$ both respond to the mechanical properties of the extracellular matrix (ECM),[15,22] while $\alpha_5\beta_1$ exhibits higher mobility[33] and initiates stronger adhesive contacts than $\alpha_v\beta_3$.[32]

A different perspective to understanding cell adhesion processes has involved the development of artificial substrates as model systems to investigate the roles of different material properties.[27] Examples include substrates with control over ligand density,[28,29] ligand patterning,[5,7] and elastic modulus.[14] The use of artificial substrates as model systems is a compromise to the true biophysical and biochemical character of the native ECM. In particular it is challenging to create artificial substrates that (i) can be actively remodeled by cell-generated forces, (ii) lack any predefined spatial patterns, and (iii) allow for dynamic presentation of ligands. The importance of these aspects of the ECM has already been recognized,[1,20] motivating the choice of self-assembled polymer films as cell substrates.

Here we investigate the role of $\alpha_5\beta_1$ and $\alpha_v\beta_3$ integrins on cell spreading and polarization when the substrates are self-assembled, laterally mobile, polymer films. The films were fabricated to present a non-fouling background surface[26] and with sufficient ligand (RGD) density to engage integrin receptors.[24] The film lateral mobilities (i.e., in-plane diffusion coefficients) D were tuned by trace addition of a small hydrophobic polymer during the self-assembly, so as to introduce viscous character into our substrates. While the role of the elastic component of cell substrates has been extensively investigated,[14,39,40,43] the viscous component has generally not been studied, even though it is a known property of the native ECM.[3,6] We find that mouse fibroblasts seeded onto our polymer films adhere and spread due to RGD-integrin binding, and more interestingly we have discovered a previously unknown relationship between integrin engagement and substrate mobility. Our results indicate that cells can sense the viscous character of cell substrates, and therefore underscore the opportunity for increasingly sophisticated materials to extend our understanding of cell adhesion processes.

MATERIALS AND METHODS

Materials

Poly(butylene)-*b*-poly(ethylene oxide) (PB-PEO) of $M_w = 10.2$ kg/mol (PDI = 1.14) and $w_{EO} = 0.39$

Address correspondence to Harry Bermudez, Department of Polymer Science and Engineering, University of Massachusetts, Amherst, MA, USA. Electronic mail: bermudez@umass.edu

resulted by hydrogenation of the commercially available 1,2-polybutadiene-*b*-poly(ethylene oxide) [$M_w = 10$ kg/mol, PDI $= 1.15$ and $w_{EO} = 0.40$, Polymer Source, Inc. (Canada)]. Poly(isobutylene) (PIB) of $M_w = 0.9$ kg/mol and PDI $= 1.3$ was also purchased from Polymer Source, Inc. (Canada). The PB-PEO copolymer terminal groups were subsequently modified to display the cell-adhesive tetrapeptide RGDS as described in,[24] and the resulting copolymer is hereafter referred to as PB-PEO-RGDS. Bovine serum albumin (BSA) was purchased from Sigma and used as received. Glass coverslips were purchased from Fisher. Trypsin-EDTA solution, Dulbecco's modified Eagle's medium (DMEM), penicillin–streptomycin solution, and calf bovine serum were supplied from ATCC. Mouse monoclonal antibodies to β_3 (2C9.G3) and $\alpha_5\beta_1$ (BMA5) were purchased from eBioscience and Millipore, respectively.

Fabrication of Supported Block Copolymer Films

Glass coverslips were rinsed with ethanol and reverse-osmosis water, subjected to oxygen plasma treatment, and submerged in the reverse-osmosis water subphase of a Langmuir trough. Chloroform solutions of polymers were applied dropwise at the air/water interface and left quiescent for 15 min before compression. The initial surface pressure after the addition of polymer solution and before compression was between 20 and 22 mN/m. The interfacial films were compressed at a rate of 10 mm/min up to a surface pressure of 39 mN/m.

For the fabrication of supported monolayers, we used chloroform solutions of PB-PEO or its mixture with PIB homopolymer. Interfacial films were transferred from the air/water interface to the glass coverslips at a constant deposition pressure and rate (39 mN/m, 1–2 mm/min) using Langmuir–Blodgett (LB) deposition. Within an hour post-fabrication, the supported monolayers were used to create a supported bilayer by the Langmuir–Schaefer (LS) technique. LS deposition was allowed a contact time of one minute between the supported monolayer and the interfacial film of PB-PEO.

For the cell adhesion studies, chloroform solutions of PB-PEO and PB-PEO–RGDS were premixed in a stoichiometric ratio that resulted in the desired RGD spacing of 50 nm. The calculation of the RGD spacing assumes ideal mixing between the polymer chains and employs the deposition surface density. The interfacial film containing PB-PEO-RGDS was introduced as the topmost layer through LS deposition onto neat and PIB-doped PB-PEO monolayers.

Cell Studies

Synchronized and enzymatically recovered fibroblasts were centrifuged (125 g, 10 min, 2×) and then resuspended in complete DMEM. The reverse-osmosis water phase above freshly prepared polymer films was exchanged with PBS solution (3×, 5 mL). PBS was exchanged with BSA solution (1 mg/mL, pH 7.4) (3×, 5 mL) and left quiescent for film passivation ($T = 20$ °C, $t = 30$ min). Afterwards, the BSA solution was exchanged with complete DMEM (3×, 3 mL). The cell suspension was added above the bilayer films to an initial surface concentration of 1.5×10^4 cells/cm^2 and placed for incubation at $T = 37$ °C and 5% CO_2. Image acquisition for all the different incubation conditions was performed at regular intervals using an Olympus IX70 inverted microscope.

To examine the role of integrins on spreading dynamics we used the specific monoclonal inhibitory antibodies (2C9.G3[25] and BMA5[18] for the extracellular domains of $\alpha_v\beta_3$ and $\alpha_5\beta_1$, respectively). Cell suspension of 1.5×10^4 cells/ml was mixed with 20 μL (0.5 mg/mL) of $\alpha_v\beta_3$ specific antibody (or 5 μL of $\alpha_5\beta_1$ antibody solution, 5 mg/mL) for 30 minutes and then it was added over DMEM-covered bilayer films to a final volume of 1 mL. Equal amounts of $\alpha_v\beta_3$ (20 μL, 0.5 mg/mL) inhibitory antibodies (or 5 μL of $\alpha_5\beta_1$ antibody solution, 5 mg/mL) were added to the seeding medium after image acquisition.

The pharmacological experiments with ROCK inhibitor (Y-27632) were performed on cells adherent on low and high mobility films for 24 h. Y-27632 was dissolved in PBS (pH 7.4) and added at a final concentration of 50 μM. Cells remained incubated with Y-27632 for 30 min before acquisition of bright field images.

Immunofluorescence Staining

After a seeding period of 24 h, cells underwent fixation by transferring the coverslips to wells containing 4% formaldehyde (Carson-Millonig Formulation; Fisher Scientific) in PBS containing Ca^{2+} and kept at ambient temperature for 15–20 min. Following three rinses with PBS, free aldehydes were quenched with 0.3 M glycine in PBS (3×, 15 min) and cells permeabilized with 0.1% Triton X-100 for 5 min. To block non-specific interaction, 2% BSA in PBS was added and incubated for 60 min at ambient temperature. Cells were rinsed with 0.1 M EDTA in PBS (3×, 5 min) to remove trace metals. Anti-vinculin-FITC (1:50 dilution, Sigma Aldrich) was added and left in the dark for 60 min at room temperature. After rinsing with 0.1% Triton X-100 in PBS (3×, 2 min) and 0.1 M EDTA in PBS (3×, 5 min), actin-phalloidin-orange (1 unit; Molecular Probes) (2% BSA) in PBS was added for 30 min. The coverslips were mounted on microscope slides with ProLong antifade reagent

(Molecular Probes) and left to cure overnight in the dark prior to image acquisition.

Statistics

Unless otherwise noted, data are reported as mean values and error bars as the standard error of the mean. For pair-wise comparisons we used the Student's *t* test.

RESULTS AND DISCUSSION

Mouse fibroblasts seeded onto our polymer films do not simply wet their substrates in a non-specific manner, they engage available RGD ligands and demonstrate anisotropic cell spreading (Supplementary Figures S1 and S2). We have previously shown that in the absence of RGD ligands, cells do not appreciably spread on these substrates.[24] In the process of adhesion and spreading, we find that cells preferentially use distinct integrins depending on the mobility of the underlying substrate. On low mobility films ($D_{\mathrm{PB-PEO}} \approx 1 \times 10^{-10}$ cm^2/s[24]), blocking $\alpha_v\beta_3$ results in significantly lower cell area A as compared to the untreated control (Fig. 1a). Conversely, on high mobility films ($D_{\mathrm{PB-PEO}} \approx 4 \times 10^{-10}$ cm^2/s[24]), blocking $\alpha_5\beta_1$ results in significantly lower cell area as compared to the untreated control (Fig. 1b). The preference for certain integrins is clear because blocking $\alpha_5\beta_1$ on low mobility films, or blocking $\alpha_v\beta_3$ on high mobility films, does not substantially inhibit cell spreading. From these endpoint results we define "critical" integrins to be $\alpha_v\beta_3$ on low mobility films and $\alpha_5\beta_1$ on high mobility films.

In previous work we showed that on low mobility films, spreading is particularly favored by a response mediated by focal adhesions (FAs),[24] and here we find that $\alpha_v\beta_3$ is primarily responsible for spreading. The connection between these results is seen by the formation of FAs with relatively large size on low mobility films (Fig. 2, black). This finding is consistent with the observed accumulation of $\alpha_v\beta_3$ in FAs[41,44] and their contributions to the formation of large FAs.[34] On high mobility films, spreading is particularly favored by a response associated with integrin ligation and clustering,[24] and here we find that $\alpha_5\beta_1$ is primarily responsible for spreading. In addition, cell adhesion on high mobility films results in the formation of FAs with smaller size (Fig. 2, gray). This finding is also consistent with the observed participation of $\alpha_5\beta_1$ in the formation of small FAs.[34] Furthermore, Rossier *et al.*[33] studied integrin diffusion both inside and outside FAs, finding that $\alpha_5\beta_1$ is always more mobile than $\alpha_v\beta_3$. Therefore our data suggest that cells transduce substrate mobility into cell spreading by selectively engaging either $\alpha_5\beta_1$ or $\alpha_v\beta_3$ integrin receptors.

Cells display the same preferential use of critical integrins to polarize their shape on films of varying mobility. To quantify cell polarization, we use the dimensionless ratio of circularity $C = P^2/4\pi A$ where P is the cell perimeter. Note that $C = 1$ corresponds to a circle (i.e., a rounded cell) and $C = 0$ corresponds to a line (i.e., a highly elongated cell). On low mobility films, blocking $\alpha_v\beta_3$ causes a large increase in circularity as compared to controls (Fig. 3a), whereas on high mobility films, blocking $\alpha_5\beta_1$ causes the largest increase in circularity (Fig. 3b). Several groups have reported cell polarization to be proportional to the overall force generated at the cell-substrate interface.[21,31] As mentioned already, low and high mobility films favor the $\alpha_v\beta_3$- and $\alpha_5\beta_1$-mediated formation of large and small FAs, respectively. Because FAs are transmitters of force onto the extracellular substrate,[35] cellular force transmission onto the films is therefore supported primarily by either $\alpha_5\beta_1$ or $\alpha_v\beta_3$. Thus our data suggest that cells transduce substrate mobility into force transmission through integrin-specific control of contractile forces.

From the data in Figs. 1 and 3, it appears that there is a minimal role for the "non-critical" integrins (i.e., $\alpha_5\beta_1$ on low mobility films and $\alpha_v\beta_3$ on high mobility films). To obtain insight into the contributions of these non-critical integrins, spreading and polarization dynamics were analyzed. Data over 24 hours were normalized and fit by sigmoidal expressions (Eqs. 1 and 2)[2,16,37] to extract global spreading and polarization rates (k_A and k_C, respectively). Based on this analysis, spreading and polarization dynamics are dominated by an intermediate regime defined by $\tau < t < \tau'$ (obtained by first-order expansion about the respective t^* in Eqs. 1 and 2, see Supplemental Material for details). Indeed, the intermediate regime of spreading area is nearly linear against time, consistent with the scaling analysis of Cuvelier *et al.*[10]

$$N(A) = \frac{A_t - A_0}{A_\infty - A_0} = \frac{1}{1 + \exp(-k_A(t - t_A^*))}, \quad (1)$$

$$N(C) = \frac{C_t - C_\infty}{C_0 - C_\infty} = 1 - \frac{1}{1 + \exp(-k_C(t - t_C^*))}. \quad (2)$$

Our analysis reveals roles for non-critical integrins in the dynamics of cell spreading and polarization. When the non-critical integrin is blocked, the spreading rate k_A decreases (Fig. 4a), with the difference more prominent on low mobility films (Table 1). To understand this result, we recall that in the absence of

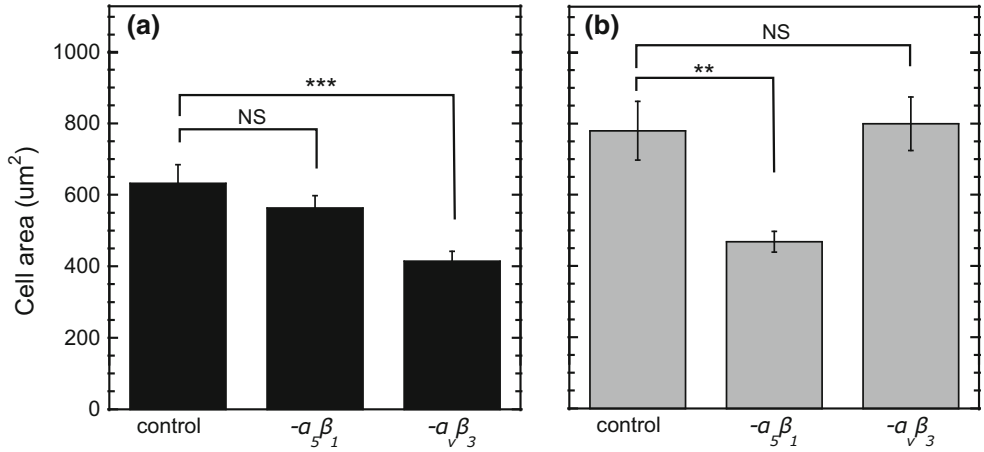

FIGURE 1. Cell area *A* on (a) low and (b) high mobility films with various blocking treatments, after 24 h. The number of cells analyzed for each condition varied from $n = 20–40$. Statistical comparison by Student's *t* test (* $p < 0.05$; ** $p < 0.01$; *** $p < 0.001$; and NS: not significant).

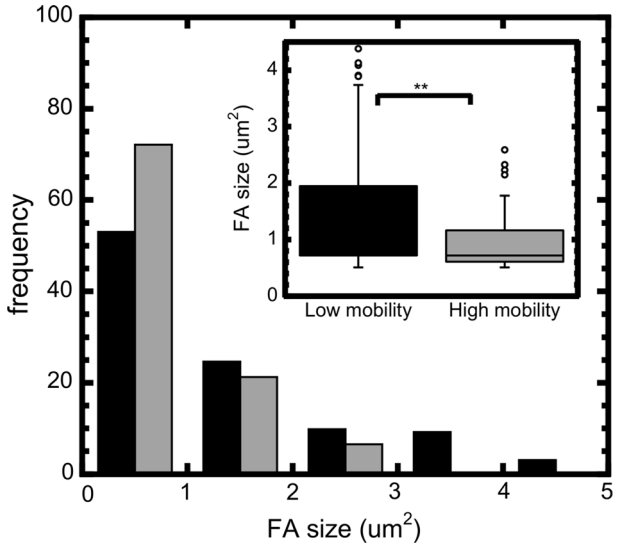

FIGURE 2. Distribution of FA size at 24 h for fibroblasts on low (black) and high (gray) mobility films, respectively. The statistical significance is shown by the inset box-and-whisker plot ($p < 0.01$). The sample size of FAs in both films is $n > 60$. Due to the limitation of optical resolution we apply a lower size cut-off of 0.5 μm^2.**

blocking antibodies cells can use both $\alpha_v\beta_3$ and $\alpha_5\beta_1$ receptors to bind adhesive ligands, whereas when either $\alpha_5\beta_1$ or $\alpha_v\beta_3$ are blocked, cells require additional time to circulate the lower number of available integrins, thus slowing cell spreading dynamics.

The effects of non-critical integrins on cell polarization dynamics are different than from cell spreading. Blocking $\alpha_5\beta_1$ on low mobility films causes an increase in the polarization rate k_C (Fig. 4b). This result is unexpected, and points to a competition between critical and non-critical integrins to determine polarization dynamics on low mobility films, which we discuss below. On the other hand, blocking $\alpha_v\beta_3$ on high mobility films does not alter the k_C significantly (Table 1), suggesting that on high mobility films $\alpha_5\beta_1$ is primarily responsible for polarization dynamics. We emphasize that these conclusions would not be anticipated from the endpoint data of Fig. 3.

The spreading lag time τ_A constitutes the period of minimal spreading at the beginning of cell-substrate contact, during which integrins bind and cluster adhesive ligands.[11,17] On both low and high mobility films, controls exhibit shorter spreading lag times (i.e., lower τ_A values) compared to either blocking treatment (Table 2), and these results can also be rationalized by the availability of multiple integrins in the control condition.

Polarization lag times τ_C are always reduced when the non-critical integrins are blocked, indicating an earlier onset of cell polarization (Table 2). This result is in contrast to the result for spreading lag times and points to the mechanistic differences between changing cell area (spreading) and changing cell shape (polarization). Indeed, the changes in τ_C suggest an interplay between $\alpha_5\beta_1$ and $\alpha_v\beta_3$ in controlling polarization dynamics. We were therefore motivated to examine the role of intracellular cues affecting cell polarization.[12] It is already known that the synergy between $\alpha_5\beta_1$ and $\alpha_v\beta_3$ increases RhoA/ROCK activity,[34] which in turn initiates signals that reduce cell polarization (i.e., increase circularity).[8] To test the possible role of ROCK on cell polarization in our system, we measured circularity C after administration with an inhibitor (Y-27632) of ROCK activity.[13,23,42] Our results on both low and high mobility films (Fig. 5) show that inhibition of ROCK activity decreases cell circularity,

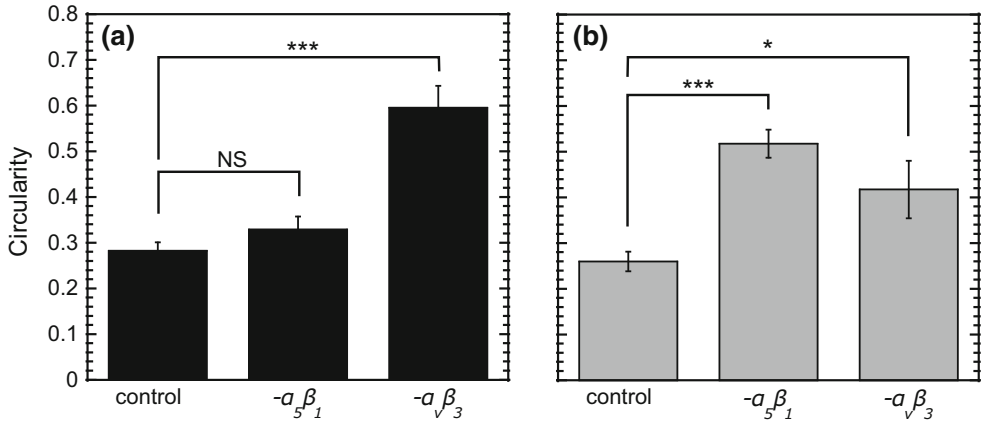

FIGURE 3. Cell circularity *C* on (a) low and (b) high mobility films with various blocking treatments, after 24 h. The number of cells analyzed for each condition varied from *n* = 20–40. Statistical comparison by Student's *t* test (* $p < 0.05$; ** $p < 0.01$; *** $p < 0.001$; and NS: not significant).

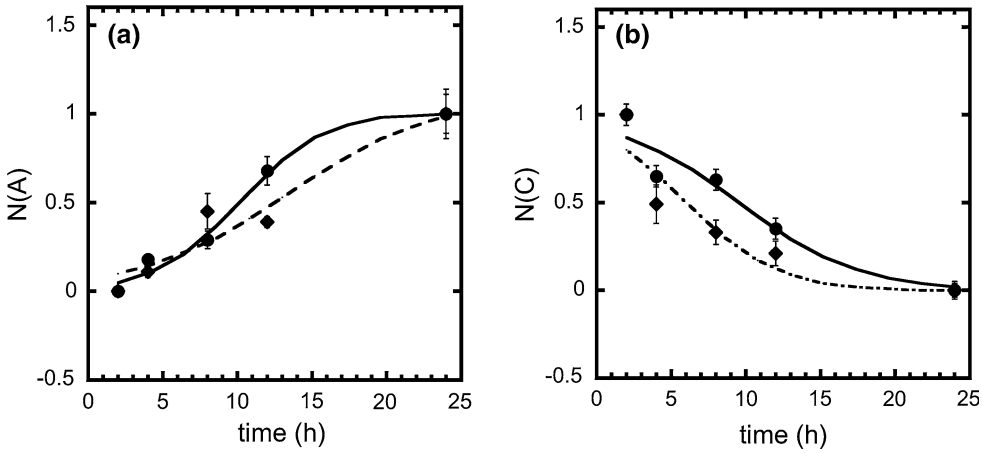

FIGURE 4. Normalized (a) cell area $N(A)$ and (b) cell circularity $N(C)$ over time on low mobility films. Diamond symbols correspond to $\alpha_5\beta_1$ blocking and circles correspond to the control condition (i.e., no blocking). The sigmoidal fits (Eqs. 1 and 2) are represented by lines. The number of cells analyzed for each blocking condition varied from *n* = 10–40.

TABLE 1. Spreading k_A and polarization k_C rates (1/h).

	Low mobility films		
	Control	$-\alpha_5\beta_1$	$-\alpha_v\beta_3$
Spreading rate k_A	0.36	0.23	n/a
Polarization rate k_C	0.25	0.34	n/a
	High mobility films		
	Control	$-\alpha_5\beta_1$	$-\alpha_v\beta_3$
Spreading rate k_A	0.42	n/a	0.39
Polarization rate k_C	0.25	n/a	0.24

All quantities are obtained from best-fits of Eqs. (1) and (2). Cases not applicable are denoted by n/a.

TABLE 2. Lag times for spreading τ_A and polarization τ_C (h).

	Low mobility films		
	Control	$-\alpha_5\beta_1$	$-\alpha_v\beta_3$
Spreading lag time τ_A	5.3	5.6	n/a
Polarization lag time τ_C	4.2	2.5	n/a
	High mobility films		
	Control	$-\alpha_5\beta_1$	$-\alpha_v\beta_3$
Spreading lag time τ_A	7.7	n/a	8.9
Polarization lag time τ_C	4.7	n/a	3.7

All quantities are obtained from best-fits of Eqs. (1) and (2). Cases not applicable are denoted by n/a.

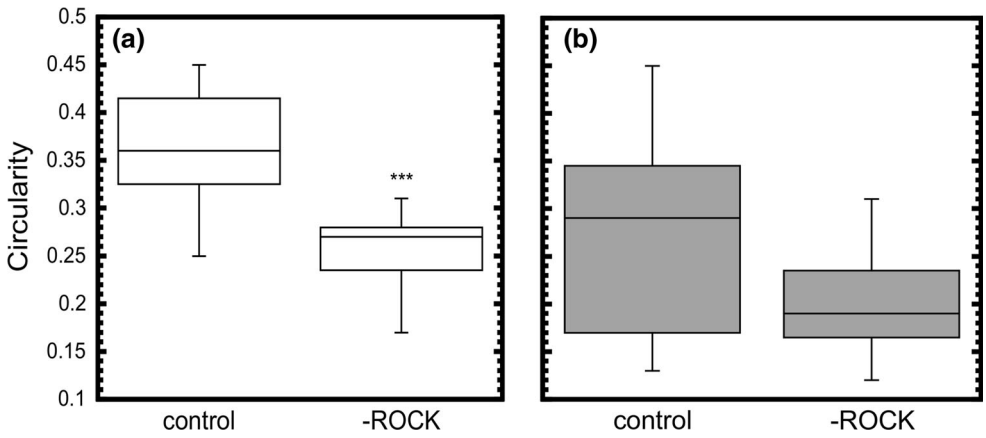

FIGURE 5. Cell circularity *C* on (a) low and (b) high mobility films after treatment with a pharmacological inhibitor of ROCK activity at 24 h.

corresponding to an increase of cell polarization. Therefore the interplay between $\alpha_5\beta_1$ and $\alpha_v\beta_3$ to promote RhoA/ROCK activity appears to explain the smaller polarization rates k_C and larger lag times τ_C for the control conditions (Tables 1 and 2).

Taken together, our results indicate that cells can sense the viscous character of cell substrates, and utilize distinct integrin receptors to promote cell adhesion, spreading, and polarization. Due to the submicron thickness of our films,[24,26] the elastic component of our substrates is only well defined in the direction normal to the substrate. Previous works[36] have shown that cells will "feel" the underlying glass coverslip in this sub-micron regime. Thus cells on our films are probing an elastic response in the normal direction and a viscous response in the lateral direction. The biological relevance of the substrate viscous properties should be viewed in a similar light to the relevance of densely crosslinked polyacrylamide gels, the "standard" for many studies[14,39,40,43] exploring the relationship between substrate elastic properties and cell behavior. In other words, the polymer films used here are *models* to represent a part of the spectrum of mechanical properties (ranging from purely fluid to purely elastic), that will ultimately will inform future studies attempting to more closely mimic physiological, or even pathological states,[4] of the heterogeneous ECM.

CONCLUSIONS

By using self-assembly we created laterally mobile polymer films to recapitulate both the display of cell-adhesive ligands and the viscous character of the native ECM. Investigating the role of integrin receptors on cell spreading and polarization reveals the relationship between cell mechano-biology and the mobility of the extracellular substrate. Specifically, $\alpha_5\beta_1$ and $\alpha_v\beta_3$ induce substrate mobility-dependent effects on cell spreading area and polarization. The extents of cell spreading and polarization are mainly affected by the mobility of integrins, presumably relative to the mobility of the substrate. While cell spreading dynamics are determined by the availability of integrins, cell

polarization dynamics are determined by integrin-mediated intracellular signaling, thus highlighting specific molecular pathways to investigate in future studies. This work emphasizes the need for increasingly sophisticated materials in order to more clearly reveal the physics of receptor-mediated cell adhesion.

ELECTRONIC SUPPLEMENTARY MATERIAL

The online version of this article (doi: 10.1007/s12195-015-0394-7) contains supplementary material, which is available to authorized users.

ACKNOWLEDGMENTS

We thank S. Peyton, T. Barker, and D. Discher for helpful discussions. We acknowledge the NSF for financial support (DMR-0847558) and the MRSEC at UMass-Amherst (DMR-0820506) for use of their facilities.

CONFLICT OF INTEREST

A.P.K. and H.B. declare that they have no conflict of interest.

STATEMENTS OF HUMAN AND ANIMAL RIGHTS AND INFORMED CONSENT

No human or animal studies were carried out by the authors for this article.

REFERENCES

[1]Antia, M., G. Baneyx, K. E. Kubow, and V. Vogel. Fibronectin in aging extracellular matrix fibrils is progressively unfolded by cells and elicits an enhanced rigidity response. *Faraday Discuss*. 139:229–249; discussion 309–25, 419–20, 2008.

[2]Bardsley, W. G., and J. D. Aplin, Kinetic analysis of cell spreading. I. Theory and modelling of curves. *J. Cell Sci.* 61:365–373, 1983.

[3]Boettiger, D. Mechanical control of integrin-mediated adhesion and signaling. *Curr. Opin. Cell Biol.* 24:592–599, 2012.

[4]Cao, L., M. K. Zeller, V. F. Fiore, P. Strane, H. Bermudez, and T. H. Barker, Phage-based molecular probes that discriminate force-induced structural states of fibronectin in vivo. *Proc. Natl. Acad. Sci USA* 109:7251–7256, 2012.

[5]Chen, C., M. Mrksich, S. Huang, G. Whitesides, and D. Ingber, Geometric control of cell life and death. *Science* 276:1425–1428, 1997.

[6]Chen, W. Y., and G. Abatangelo. Functions of hyaluronan in wound repair. *Wound Repair Regen*. 7:79–89, 1999.

[7]Chen, X., Y.-D. Su, V. Ajeti, S.-J. Chen, and P. J. Campagnola, Cell adhesion on micro-structured fibronectin gradients fabricated by multiphoton excited photochemistry.*Cell Mol. Bioeng*. 5:307–319, 2012.

[8]Cox, E. A., S. K. Sastry, and A. Huttenlocher, Integrin-mediated adhesion regulates cell polarity and membrane protrusion through the Rho family of GTPases. *Mol. Biol. Cell* 12:265–77, 2001.

[9]Cretel, E., A. Pierres, A.-M. Benoliel, and P. Bongrand, How Cells feel their environment: a focus on early dynamic events. *Cell Mol. Bioeng*. 1:5–14, 2008.

[10]Cuvelier, D., M. Théry, Y.-S. Chu, S. Dufour, J.-P. Thiéry, M. Bornens, P. Nassoy, and L. Mahadevan, The universal dynamics of cell spreading. *Curr. Biol.* 17:694–699, 2007.

[11]Döbereiner, H.-G., B. Dubin-Thaler, G. Giannone, H. S. Xenias, and M. P. Sheetz, Dynamic phase transitions in cell spreading. *Phys. Rev. Lett*. 93:108105, 2004.

[12]Drubin, D. G., and W. J. Nelson, Origins of cell polarity. *Cell* 84:335–344, 1996.

[13]Dumbauld, D. W., H. Shin, N. D. Gallant, K. E. Michael, H. Radhakrishna, and A. J. Garcia, Contractility modulates cell adhesion strengthening through focal adhesion kinase and assembly of vinculin-containing focal adhesions. *J. Cell. Physiol*. 223:746–756, 2010.

[14]Engler, A., L. Bacakova, C. Newman, A. Hategan, M. Griffin, and D. Discher, Substrate compliance versus ligand density in cell on gel responses. *Biophys. J*. 86:617–628, 2004.

[15]Friedland, J. C., M. H. Lee, and D. Boettiger, Mechanically activated integrin switch controls alpha5beta1 function. *Science* 323:642–644, 2009.

[16]García, A. J., P. Ducheyne, and D. Boettiger, Quantification of cell adhesion using a spinning disc device and application to surface-reactive materials. *Biomaterials* 18:1091–1098, 1997.

[17]Giannone, G., B. J. Dubin-Thaler, O. Rossier, Y. Cai, O. Chaga, G. Jiang, W. Beaver, H.-G. Döbereiner, Y. Freund, G. Borisy, and M. P. Sheetz, Lamellipodial actin mechanically links myosin activity with adhesion-site formation. *Cell* 128:561–575, 2007.

[18]Gupta, S. K., and N. E. Vlahakis, Integrin alpha9beta1 mediates enhanced cell migration through nitric oxide synthase activity regulated by Src tyrosine kinase. *J. Cell Sci.* 122:2043–2054, 2009.

[19]Hynes, R., Integrins: bidirectional, allosteric signaling machines. *Cell* 110:673–687, 2002.

[20]Hynes, R. O., The dynamic dialogue between cells and matrices: implications of fibronectin's elasticity. *Proc. Natl. Acad. Sci. USA*. 96:2588–2590, 1999.

[21]Ingber, D. E., Mechanosensation through integrins: cells act locally but think globally. *Proc. Natl. Acad. Sci. USA* 100:1472–1474, 2003.

[22]Jiang, G., A. H. Huang, Y. Cai, M. Tanase, and M. P. Sheetz, Rigidity sensing at the leading edge through alphavbeta3 integrins and RPTPalpha. *Biophys. J*. 90:1804–1809, 2006.

[23]Kernochan, L., B. Tran, P. Tangkijvanich, A. Melton, S. Tam, and H. Yee, Endothelin-1 stimulates human colonic myofibroblast contraction and migration. *Gut* 50:65–70, 2002.

[24]Kourouklis, A. P., R. V. Lerum, and H. Bermudez, Cell adhesion mechanisms on laterally mobile polymer films. *Biomaterials* 35:4827–4834, 2014.

[25]Lakshmikanthan, S., M. Sobczak, C. Chun, A. Henschel, J. Dargatz, R. Ramchandran, and M. Chrzanowska-Wod-

nicka, Rap1 promotes VEGFR2 activation and angiogenesis by a mechanism involving integrin $\alpha_v\beta_3$. *Blood* 118:2015–2026, 2011.
[26]Lerum, R. V., and H. Bermudez, Controlled interfacial assembly and transfer of brushlike copolymer films. *ChemPhysChem* 11:665–669, 2010.
[27]Lutolf, M. P., and J. A. Hubbell, Synthetic biomaterials as instructive extracellular microenvironments for morphogenesis in tissue engineering. *Nat. Biotechnol.* 23:47–55, 2005.
[28]Maheshwari, G., G. Brown, D. Lauffenburger, A. Wells, and L. Griffith, Cell adhesion and motility depend on nanoscale RGD clustering. *J. Cell Sci.* 113:1677–1686, 2000.
[29]Massia, S. P., and J. A. Hubbell, An RGD spacing of 440 nm is sufficient for integrin alpha V beta 3-mediated fibroblast spreading and 140 nm for focal contact and stress fiber formation. *J. Cell Biol.* 114:1089–1100, 1991.
[30]Pierschbacher, M. D., and E. Ruoslahti, Cell attachment activity of fibronectin can be duplicated by small synthetic fragments of the molecule. *Nature* 309:30–33, 1984.
[31]Rape, A. D., W.-H. Guo, and Y.-L. Wang, The regulation of traction force in relation to cell shape and focal adhesions. *Biomaterials* 32:2043–2051, 2011.
[32]Roca-Cusachs, P., T. Iskratsch, and M. P. Sheetz, Finding the weakest link: exploring integrin-mediated mechanical molecular pathways. *J. Cell Sci.* 125:3025–3038, 2012.
[33]Rossier, O., V. Octeau, J.-B. Sibarita, C. Leduc, B. Tessier, D. Nair, V. Gatterdam, O. Destaing, C. Albigès-Rizo, R. Tampé, L. Cognet, D. Choquet, B. Lounis, and G. Giannone, Integrins ?1 and ?3 exhibit distinct dynamic nanoscale organizations inside focal adhesions. *Nat. Cell Biol.* 14:1057–1067, 2012.
[34]Schiller, H. B., M.-R. Hermann, J. Polleux, T. Vignaud, S. Zanivan, C. C. Friedel, Z. Sun, A. Raducanu, K.-E. Gottschalk, M. Théry, M. Mann, and R. Fässler, ?1- and v-class integrins cooperate to regulate myosin II during rigidity sensing of fibronectin-based microenvironments. *Nat. Cell Biol.* 15:625–636, 2013.
[35]Schwarz, U. S., N. Q. Balaban, D. Riveline, A. Bershadsky, B. Geiger, and S. A. Safran, Calculation of forces at focal adhesions from elastic substrate data: the effect of localized force and the need for regularization. *Biophys. J.* 83:1380–1394, 2002.
[36]Sen, S., A. J. Engler, and D. E. Discher, Matrix strains induced by cells: Computing how far cells can feel. *Cell Mol. Bioeng.* 2:39–48, 2009.
[37]Sen, S., and S. Kumar, Cell-matrix de-adhesion dynamics reflect contractile mechanics. *Cell Mol. Bioeng.* 2:218–230, 2009.
[38]Shankarraman, V., M. M. Shah, and M. R. Caplan, Substrates elicit different patterns of intracellular signaling which in turn cause differences in cell adhesion. *Cell Mol. Bioeng.* 3:229–246, 2010.
[39]Solon, J., I. Levental, K. Sengupta, P. C. Georges, and P. A. Janmey, Fibroblast adaptation and stiffness matching to soft elastic substrates. *Biophys. J.* 93:4453–4461, 2007.
[40]Stroka, K. M., and H. Aranda-Espinoza, Neutrophils display biphasic relationship between migration and substrate stiffness. *Cell Motil. Cytoskeleton* 66:328–341, 2009.
[41]Yamada, K. M., R. Pankov, and E. Cukierman, Dimensions and dynamics in integrin function. *Braz. J. Med. Biol. Res.* 36:959–966, 2003.
[42]Yamana, N., Y. Arakawa, T. Nishino, K. Kurokawa, M. Tanji, R. E. Itoh, J. Monypenny, T. Ishizaki, H. Bito, K. Nozaki, N. Hashimoto, M. Matsuda, and S. Narumiya, The Rho-mDia1 pathway regulates cell polarity and focal adhesion turnover in migrating cells through mobilizing Apc and c-Src. *Mol. Cell. Biol.* 26:6844–6858, 2006.
[43]Yeung, T., P. Georges, L. Flanagan, B. Marg, M. Ortiz, M. Funaki, N. Zahir, W. Ming, V. Weaver, and P. Janmey, Effects of substrate stiffness on cell morphology, cytoskeletal structure, and adhesion. *Cell Motil. Cytoskeleton* 60:24–34, 2005.
[44]Zamir, E., and B. Geiger, Molecular complexity and dynamics of cell-matrix adhesions. *J. Cell Sci.* 114:3583–3590, 2001.